

Benchmarking DIV1D on SOLPS-ITER simulations of TCV plasmas

G.L. Derks^{1,2,3}, J.P.K.W. Frankemölle^{1,3}, J.T.W. Koenders^{1,2},
M. van Berkel¹, H. Reimerdes⁴, M. Wensing⁴, E. Westerhof¹

¹DIFFER – Dutch Institute for Fundamental Energy Research, Eindhoven, Netherlands.

²Ecole Polytechnique Fédérale de Lausanne (EPFL), Swiss Plasma Center (SPC), Lausanne, Switzerland

³Eindhoven University of Technology, Control Systems Technology, Eindhoven, Netherlands

⁴Eindhoven University of Technology, Science and Technology of Nuclear Fusion, Eindhoven, Netherlands

LINK to Draft paper for PPCF: https://users.euro-fusion.org/repository/pinboard/EFDA-JET/journal/98800_ppcf_2022_gd_v13_links.pdf

48th EPS conference on plasma physics
27 June – 1 July 2022
P4b.120

DIFFER
SCIENCE FOR FUTURE ENERGY

g.l.derks@diffier.nl

Motivation and introduction

The exhaust

Heat flux q MWm^{-2}

In ITER:

- Upstream [1]:

$$q_{\parallel} \approx 100 \text{ MWm}^{-2}$$

- Target requirement [2]: q_{\parallel}

$$q_{\perp} \lesssim 15 \text{ MWm}^{-2}$$

- Solution [3]:

detachment

$$q_{\perp} \approx 10 \text{ MWm}^{-2}$$

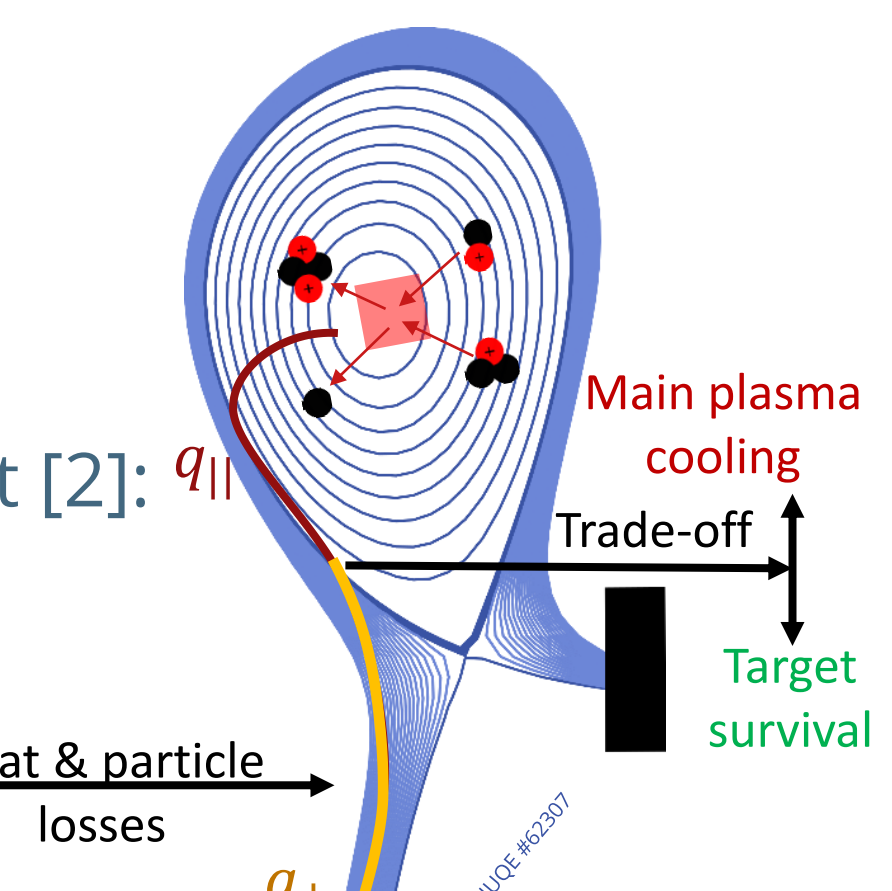


Figure 1. The heat in the core flows across the edge towards the target. There is a trade-off between target survival and core performance.

Control

Actuator

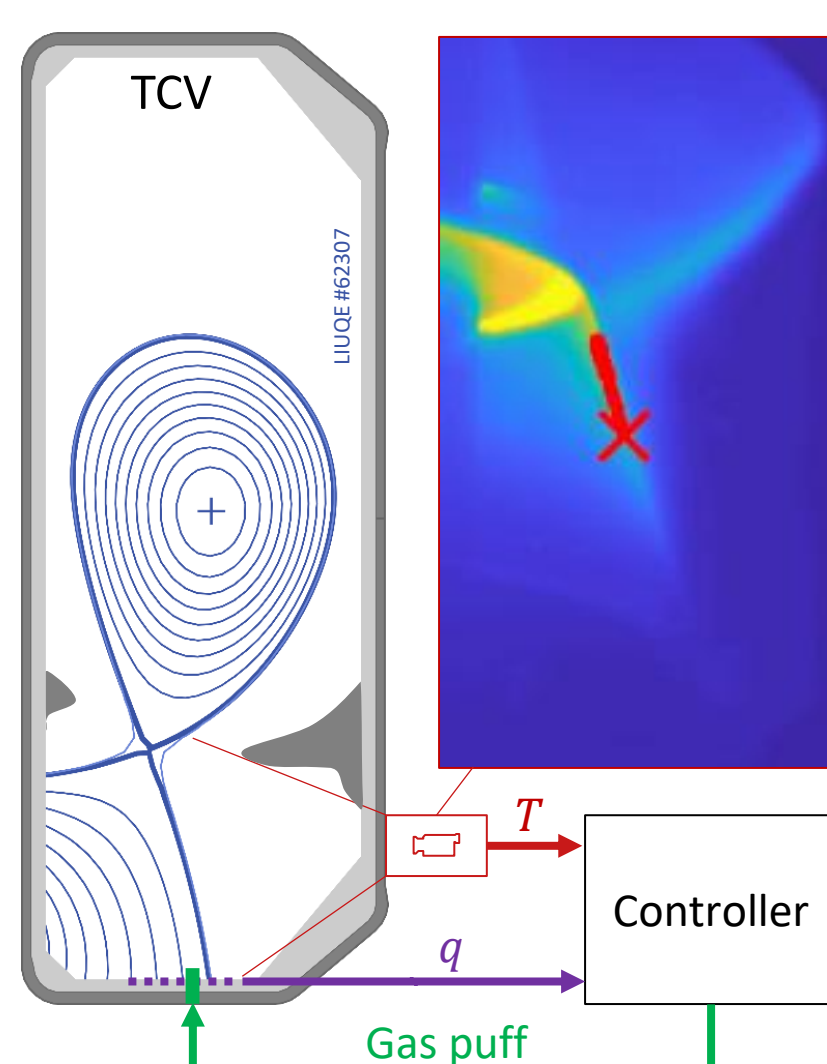
- Gas valve (puff) [4]

Sensors

- MANTIS camera (T) [5]
- Langmuir probes (q) [6]

Good controllers

- Designed with a dynamic model currently based on measurements [7,8]



Dynamic models

Envisioned role for DIV1D

- Match SOLPS-ITER equilibria
- Transition between equilibria
- Self-consistently with minimal complexity

Figure 2. Illustration of detachment control loop in the Tokamak à Configuration Variable (TCV) inspired by [5,7,8]. The MANTIS camera captures tangential C2+ emission which is an indication of plasma temperature. The Langmuir probes measure heat flux. Based on measurements, the controller decides on the amount of gas to be puffed.

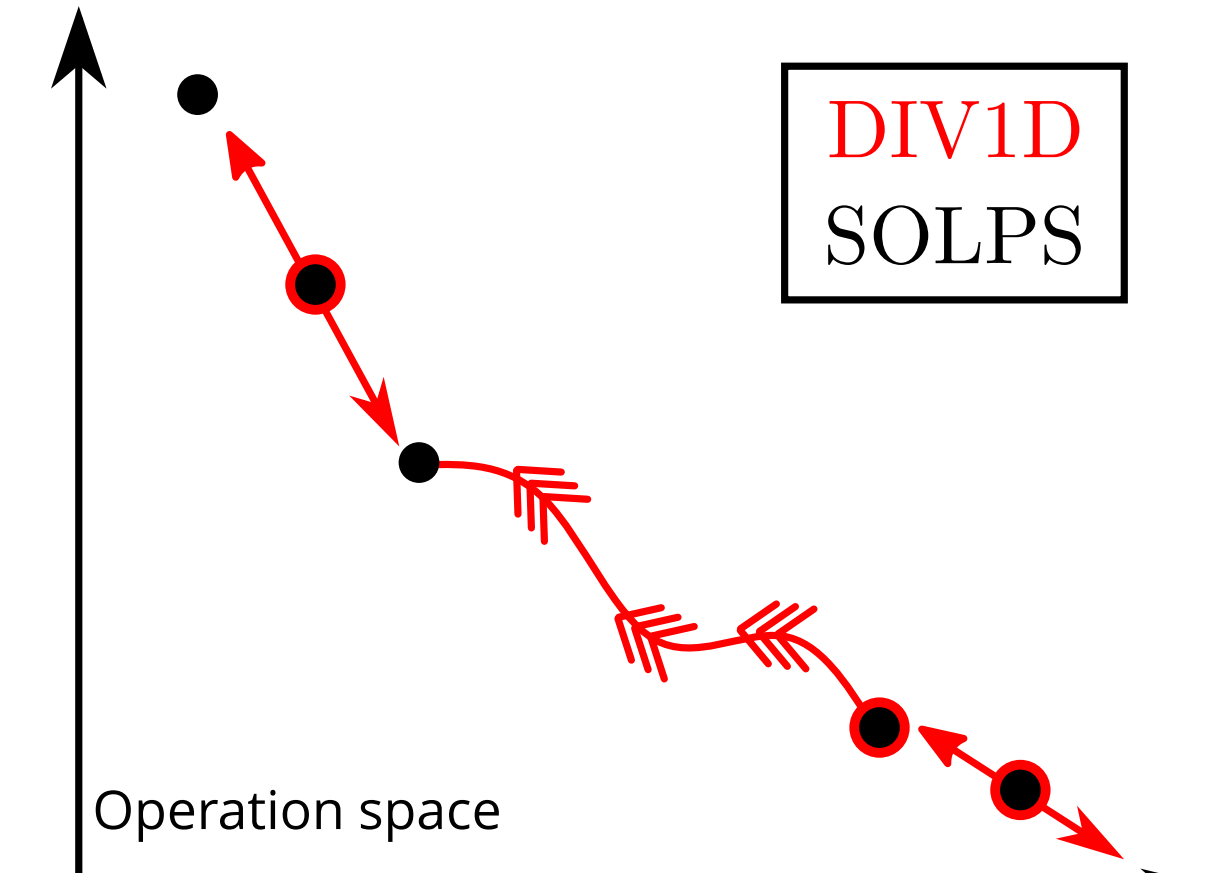


Figure 3. The operational space of the divertor plasma in which SOLPS-ITER describes static (black) operating points whereas DIV1D can dynamically (red) move around and transition between SOLPS-ITER solutions.

Models

SOLPS-ITER [9]

Combines:

- B2.5 multi-fluid plasma
- EIRENE Monte Carlo neutral

Simulated TCV plasma [10]:

- L-mode #62807
- $I_p = 250 \text{ kA} \rightarrow 360 \text{ kW}$
- Gas puff scan

Important settings:

- $D_{\perp\alpha} = 0.2, X_{\perp\alpha} = 1 \text{ (m}^2\text{s}^{-1}\text{)}$
- $\gamma \approx 5.7 \text{ (-)}, R = 0.99$

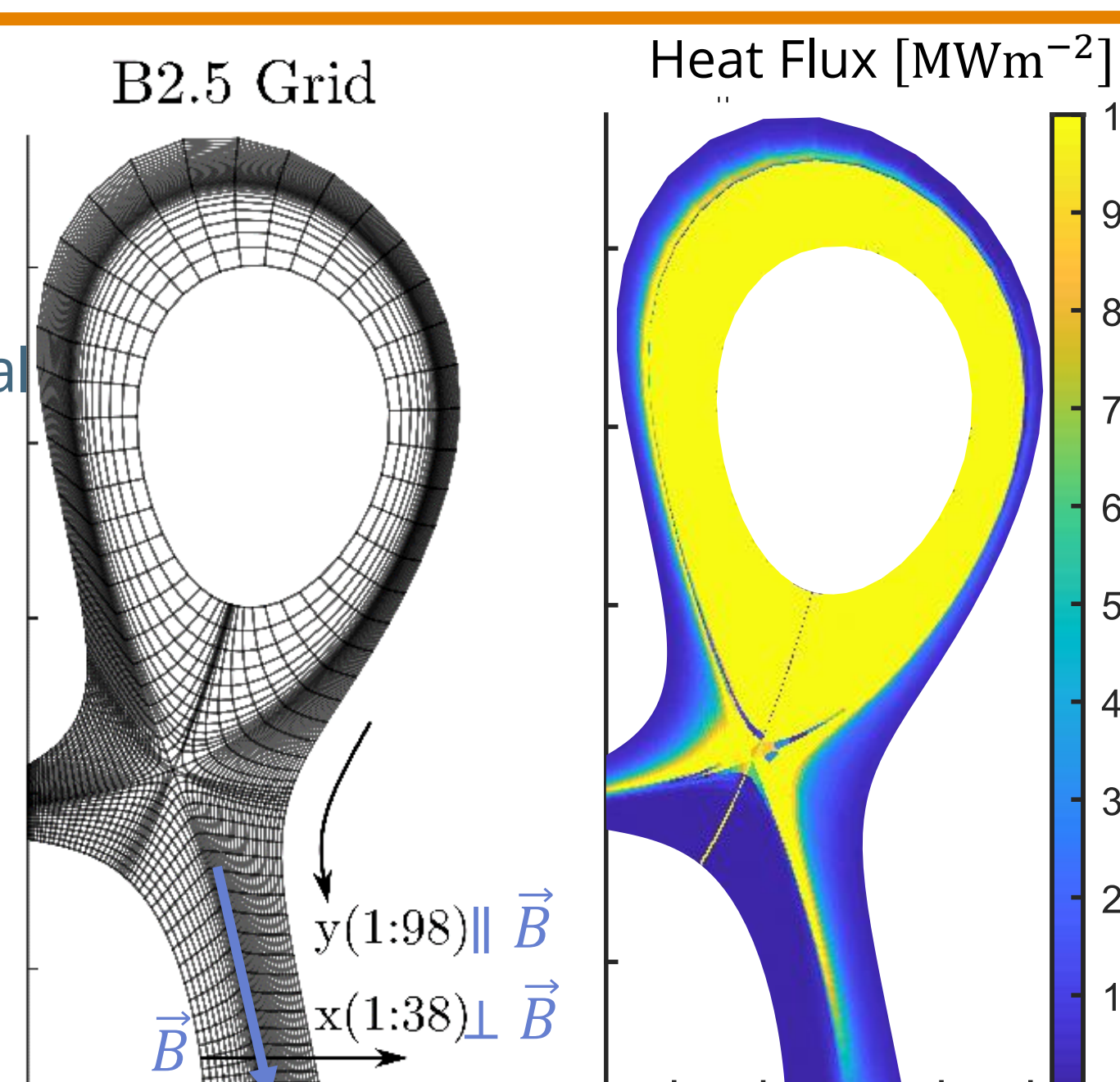


Figure 4. The B2.5 grid and parallel heat flux of SOLPS.

Models

DIV1D: a 1D dynamic divertor model [11]

Assumptions:

- $T_i = T_e$
- No radial losses

Balance equations, e.g. [12-15]:

- Particle, Momentum, Energy

Atomic processes:

- Ionization, Recombination, Charge exchange, Excitation [16], Carbon radiation [17]

Mimic cross-field transport (unique features)

- Effective heat flux expansion

- Neutral gas background

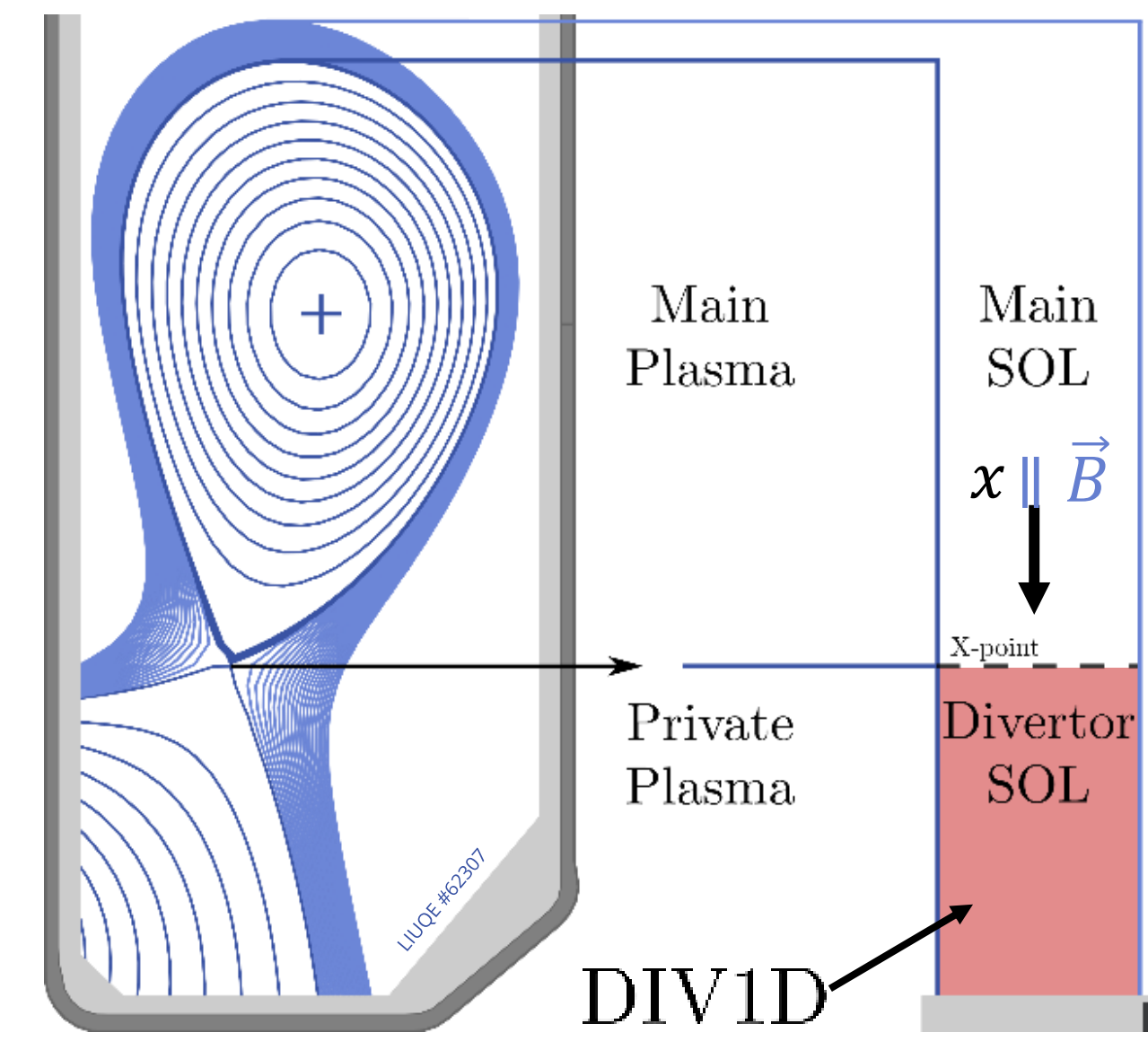


Figure 5. Dissection of poloidal cross-section. DIV1D describes the divertor scrape-off layer (SOL).

Method

Mapping SOLPS-ITER to 1D profiles

To compare, 2D solutions must be interpreted in 1D

→ Not trivial with drifts and X-points

A single flux-tube as in [13]

- Sources dominated by cross-field transport

List-Group">

- Does not represent macro divertor plasma

FWHM heat flux channel inspired on [18,19]

List-Group">

- Negligible cross-field sources on boundaries

List-Group">

- Average values represent profiles

List-Group">

- Variations indicate validity of 1D interpretation

→ 2D features of X-point difficult to interpret in 1D → upstream →

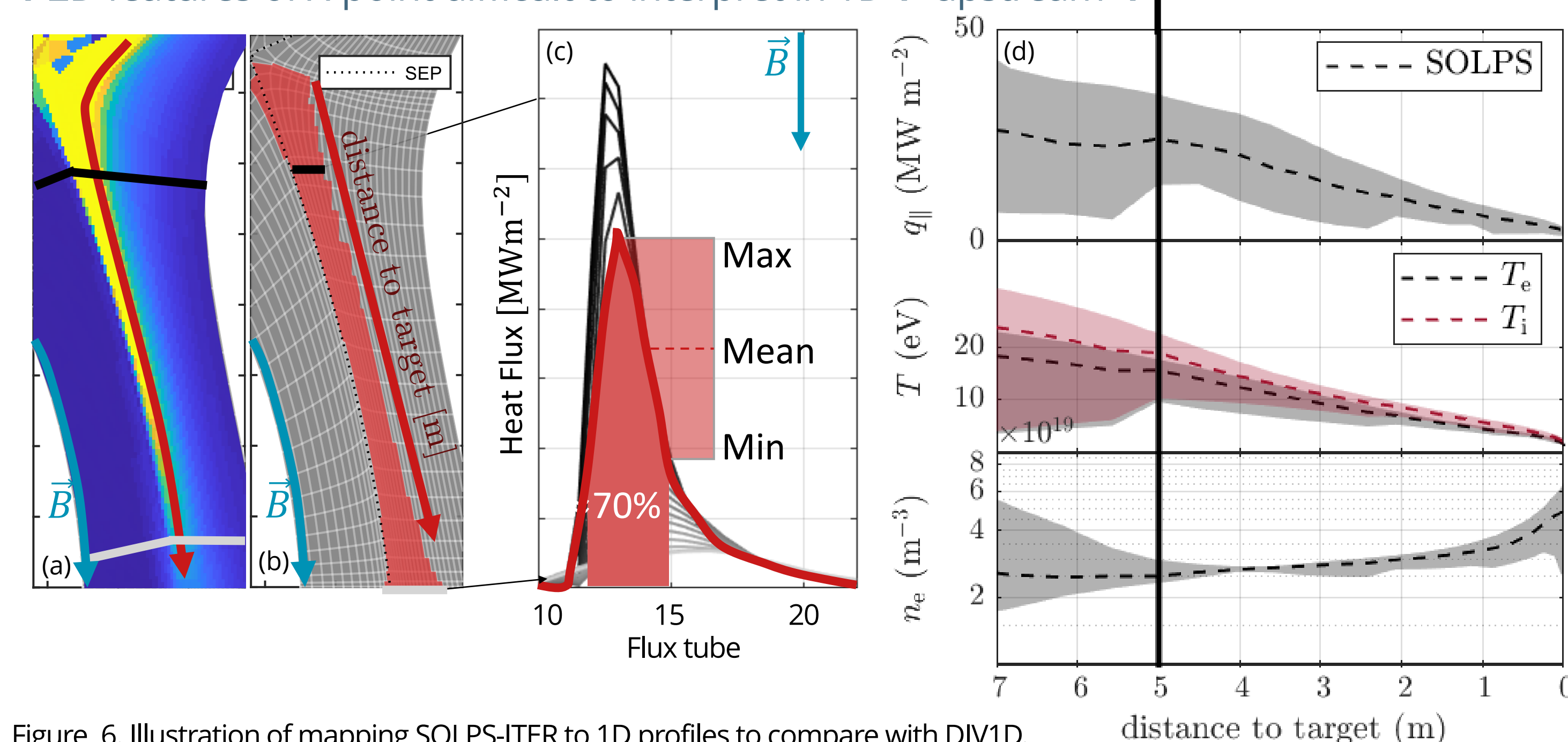


Figure 6. Illustration of mapping SOLPS-ITER to 1D profiles to compare with DIV1D.

Results

Matches and transitions between SOLPS-ITER?

Simulated DIV1D with varying upstream density $n_{e,u}$

and background gas density n_b . Other values were

fixed. The static comparison in Figure 7 for the

upstream density $n_{e,u} = 2.5 \cdot 10^{19} \text{ m}^{-3}$ shows good

agreement in plasma profiles. The biggest error is

visible in the parallel velocity. Figure 8 compares the

scalars for a range of upstream densities $n_{e,u}$,

showing the background gas density, loss fractions

$f_{\text{pwr}}, f_{\text{pwr}}$ [3], target ion flux $\Gamma_{i,t}$, and target

temperature T_t . There is good agreement in a

density range of $n_{e,u} = 1.8 - 2.7 \cdot 10^{19} \text{ m}^{-3}$.

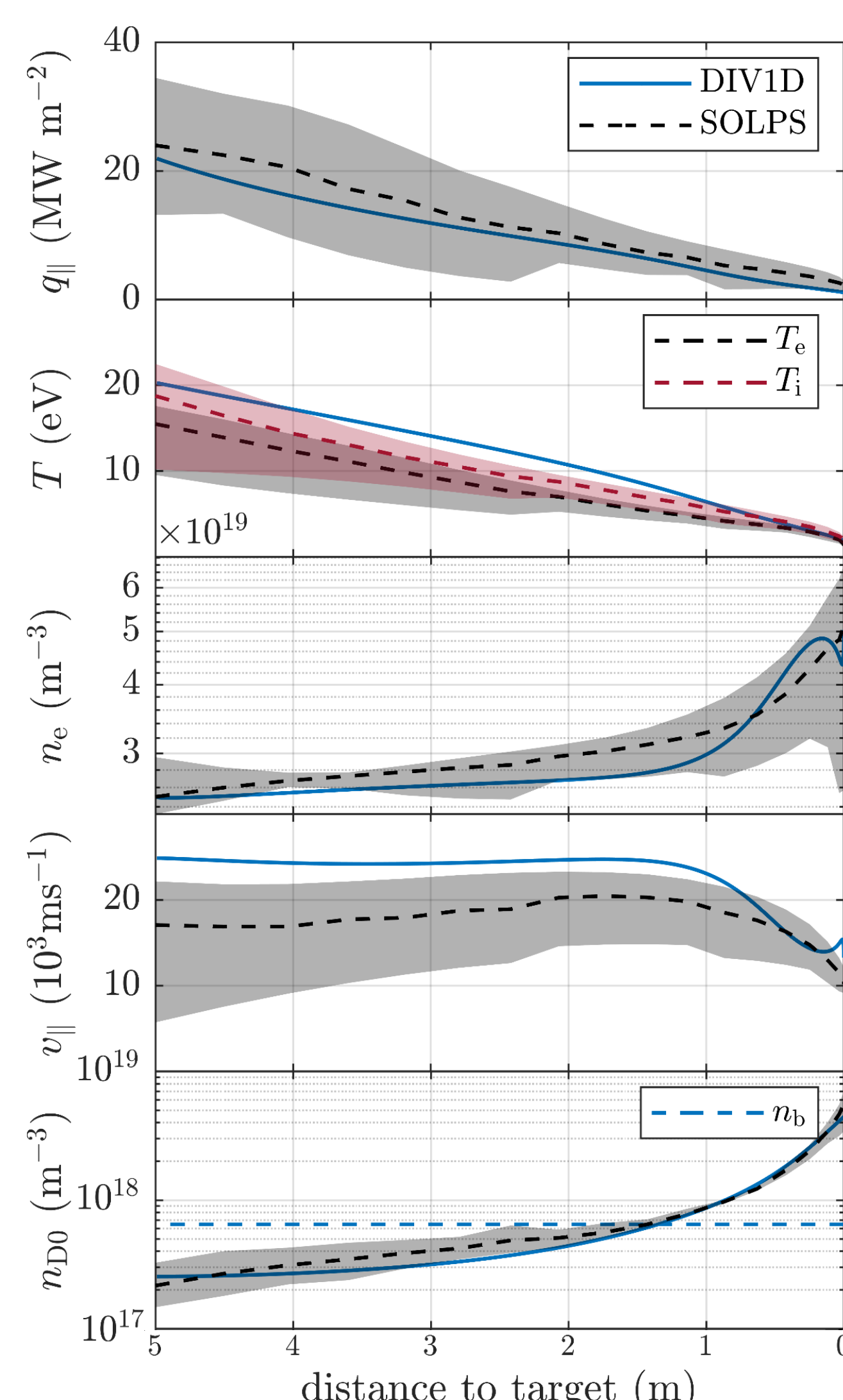


Figure 7. Comparison of 2D SOLPS-ITER solutions mapped to 1D profiles with DIV1D.

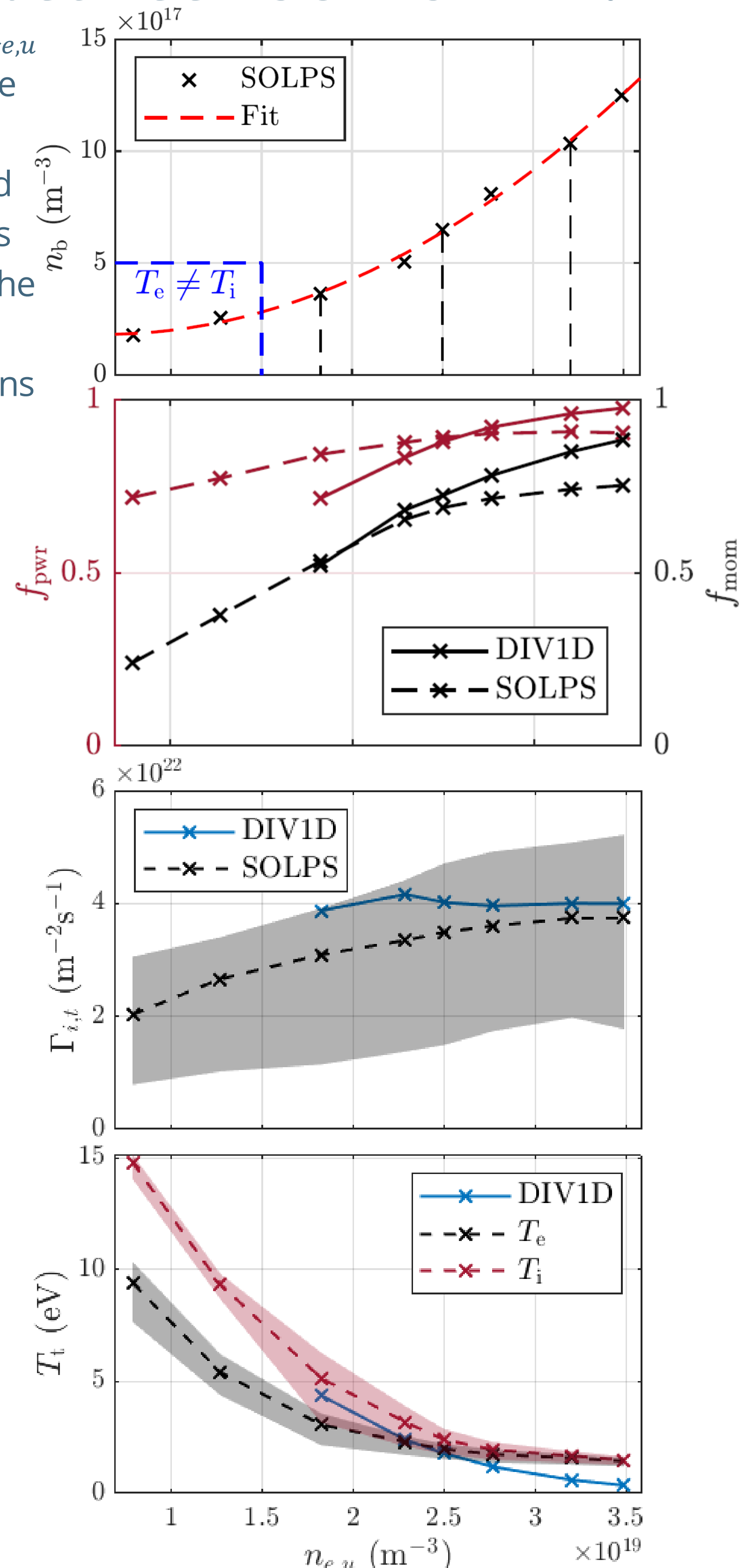


Figure 8. Comparison between mapped SOLPS solutions with DIV1D. In DIV1D we fixed $L = 5 \text{ m}, q_{\parallel,u} = 22 \text{ MW/m}^2$, $f_c = 3\%$, $\sin(\theta) = 0.6$, and the effective flux expansion $A_t/A_u = 2.3$. The upstream density and neutral background were varied.

Conclusion and Discussion

- Reasonable agreement between FWHM 1D SOLPS-ITER and DIV1D for upstream densities $n_{e,u} = 1.8 - 2.7 \text{ m}^{-3}$.
- Matching FWHM 1D SOLPS-ITER with DIV1D indicates both that DIV1D can describe the divertor plasma in 1D and that the FWHM 1D interpretation of 2D equilibria is physical.
- Discrepancies might be resolved by considering:
 - transport in radiation functions [17,20]
 - molecules [20], ExB drifts [21]
 - momentum and energy for neutrals [15]
- Future research will focus on:
 - Extending validity by resolving discrepancies
 - Reproducing on other (bigger) devices
 - Compare to measured dynamics of detachment [7,8]

References

- J. Chen et al., Phys. Plasmas **25**, 5 (2019)
- R. A. Pitts et al., Nucl. Mat. And Energy **20**, 100696 (2019)
- P. C. Stangeby, Plasma Phys. Control. Fusion **64**, 44022 (2018)
- S. Bates et al., Rev. Sci. Instrum. **55**, 6 (1984)
- A. Perek et al., Rev. Sci. Instrum. **90**, 123514 (2019)
- O. Février et al., Rev. Sci. Instrum. **89**, 053502 (2018)
- T. Ravensbergen et al., Nat. Commun. **12**, 1105 (2021)
- J. Koenders et al., Nucl. Fusion **62**, 066025 (2022)
- S. Wiesen et al., J. Nucl. Mater. **463**, 480-484 (2015)
- M. Wensing et al., Phys. Plasmas **28**, 8 (2021)
- E. Westerhof et al., 47th EPS Conf. Plasma Physics (2021)
- S. Nakazawa et al., Plasma Phys. Control. Fusion **42**, 4 (2000)
- E. Havlíčková et al., Plasma Phys. Control. Fusion **55**, 6 (2013)
- S. TOGO et al., Plasma Phys. Control. Fusion **8**, 0 (2013)
- B. D.udson et al., Plasma Phys. Control. Fusion **61**, 6 (2019)
- D. Reiter, "The EIRENE Code User Manual" Inst. Für Energ. P. 304 (2019)
- D. E. Post et al., At. Data Nucl. Data Tables **20**, 5 (1977)
- M. A. Makowski et al., Phys. Plasmas **19**, 5 (2012)
- T. Eich et al., Nucl. Fusion **53**, 9 (2013)
- K. Verhaegh et al., Nucl. Fusion **61**, 10 (2021)
- C. Tsuei et al., Plasma Phys. Control. Fusion **64**, 065008 (2022)



TU/e
EINDHOVEN
UNIVERSITY OF
TECHNOLOGY
EUROfusion

EPFL



This work has been carried out within the framework of the EUROfusion Consortium, funded by the European Union via the Euratom Research and Training Programme (Grant Agreement No 101052200 — EUROfusion). Views and opinions expressed are however those of the author(s) only and do not necessarily reflect those of the European Union or the European Commission. Neither the European Union nor the European Commission can be held responsible for them.